nature materials

SUPPLEMENTARY INFORMATION

DOI: 10.1038/NMAT3050

Supramolecular Spin Valves

M. Urdampilleta,[1] J.-P. Cleuziou,[1] S. Klyatskaya,[2] M. Ruben,[2,3*] W. Wernsdorfer[1,*]

[1] Institut Néel, associé á l'Université Joseph Fourier, CNRS, BP 166, 38042 Grenoble Cedex 9, France

[2] Institute of Nanotechnology (INT), Karlsruhe Institute of Technology (KIT), 76344 Eggenstein-Leopoldshafen, Germany

[3] Institute de Physique et Chimie de Matériaux de Strasbourg (IPCMS), CNRS-Université de Strasbourg, 67034 Strasbourg, France

Content:

1- Zeeman energy diagram for the $J = 6$ ground multiplet of $TbPc_2$

In transition metal SMM the distance between substates of the same multiplet is known to lie between 1 K and 20 K. QTM can occur when two substates are brought to resonance by the applied magnetic field. The situation is different in $TbPc_2$: the two lowest substates of the $J = 6$

DOI: 10.1038/NMAT3050

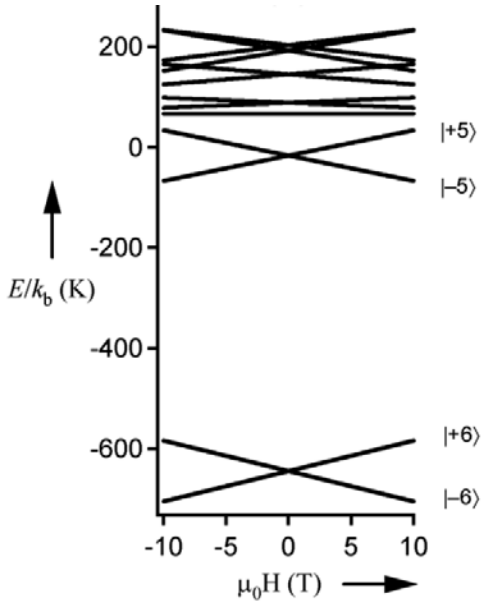

Figure S1: Zeeman Energy diagram as a function of the longitudinal field for the $J = 6$ ground multiplet (adapted from Ref. 15 of the main text). The first excited state is around 600K above the ground state.

2- Magneto-resistance of others samples

We studied about 130 samples. 25 samples showed magnetic signals due to the $TbPc_2$* molecules and seven samples were studied in detail, showing similar behaviour concerning their magneto-conductance. The three samples presented in Figure S2 were fabricated using CVD nanotubes (see Method section). Catalyst islands were designed on SiO_2 by creating holes by optical lithography in LOR3A resist, which were filled with Fe/Mo catalyst in nanoporous alumina. The samples were grown in a Firstnano CVD oven at 750°C, whereby methane is used as a carbon source. The subsequent fabrication of the quantum dot and its functionalization with SMM-$TbPc_2^*$ is described in the Method section.

Figure S2 shows that the spin-valve behaviour is easily reproducible in different batches, but the exact magneto-conductance ratio can vary from sample to sample. These differences can be related to slight local variations of the coupling between the quantum magnets and the nanotube.

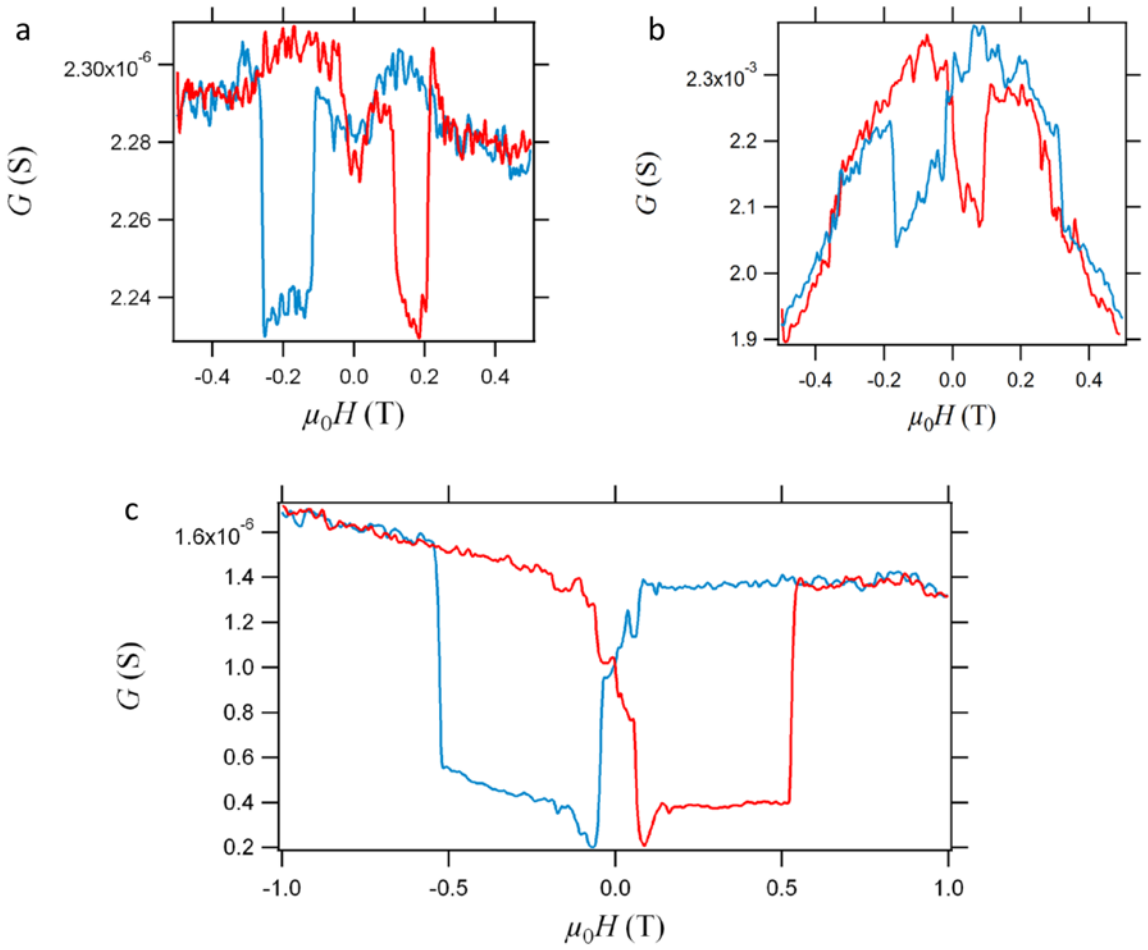

Figure S2: **Magneto-resistance of three different samples**. **a** ~2% **b**, ~10% **,** and **c** ~200% of magneto-resistance ratio, measured as a function of the magnetic field. The red and blue curves correspond to the conductance under increasing and decreasing field, respectively. The conductance jumps around zero-field are attributed to few molecules which tunnelling at avoided level crossings, while the jumps at higher field can be related to the direct relaxation process of a single molecule.

3- Orientation of the molecules on the nanotube

The angular dependence of the switching field shows in all studied samples a clear anisotropic response. In Figure S3 the hysteresis of the conductance is plotted as a function of the applied field angle for four different samples revealing clearly an easy axis of magnetisation. Because the easy axis is perpendicular to the phthalocyanines (see Fig. 1a), the orientation of the molecule with respect to the nanotube can be found and is schematically drawn in the respective insets. We found that in most of the samples the magnetic easy axes is transverse to the nanotube axis, which is in good agreement with the fact that the molecule maximizes its supramolecular interaction in the flat-landing configuration. The inset of Figure S3c shows the case in which the easy axis of the quantum magnet is in parallel to the tube axis leading to a reduced exchange coupling and a slurred device response.

DOI: 10.1038/NMAT3050

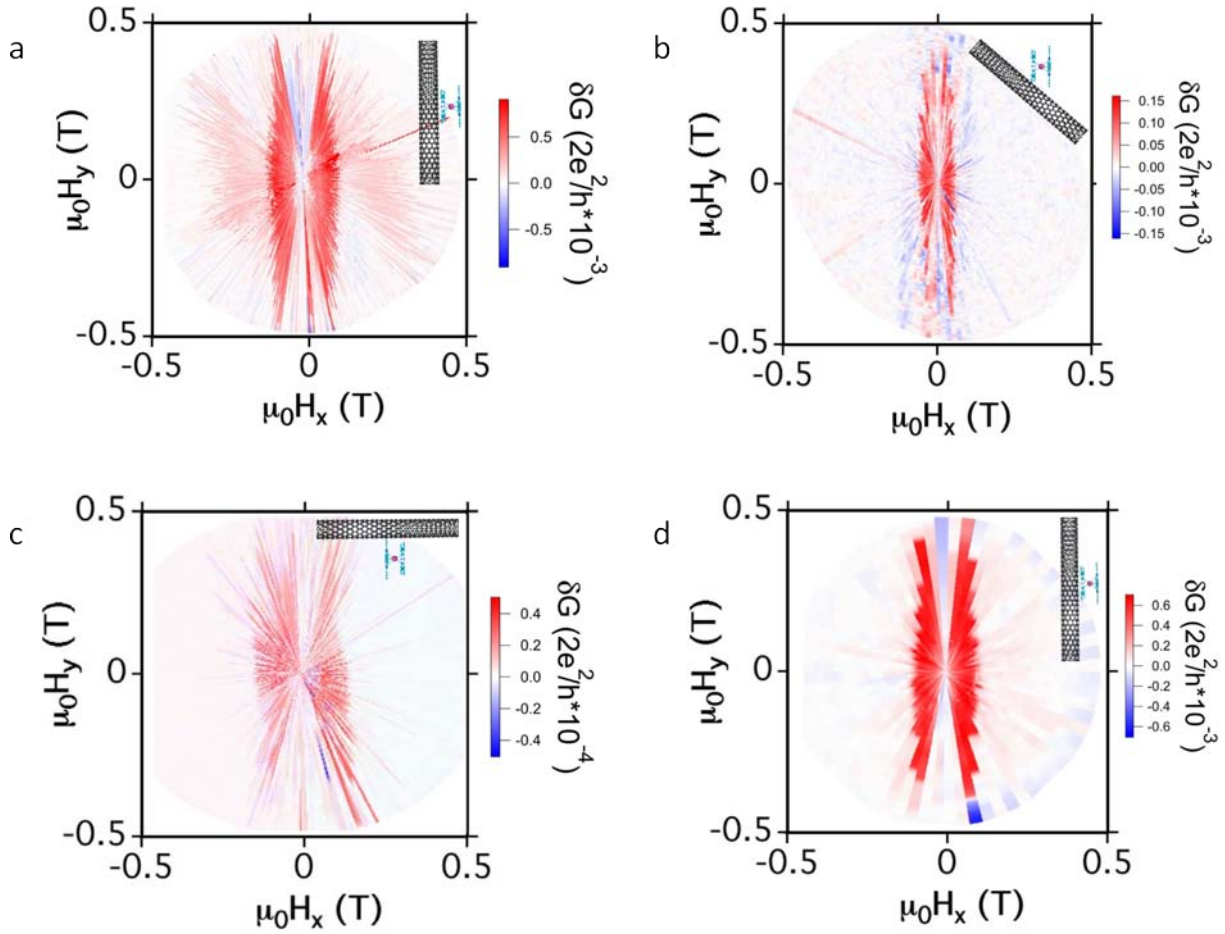

Figure S3: **a-d**, Angular dependence of the conductance hysteresis for four samples. The difference between trace (from -1 T to +1 T) and retrace (from +1 T to -1 T) is plotted as a function of the angle of the applied field. The main switching fields correspond to the direct relaxation process. It is important to note that the switching field along the hard magnetization axis (*y*-axis) cannot be measured because our magnets are limited to about 1 T. The insets depict the orientation of the $TbPc_2^*$ molecules with respect to the nanotubes. In **a**, the switching of two $TbPc_2^*$-molecules can be distinguished. The easy axis of the second one is 45° tilted from the nanotube axis and seems less coupled to the nanotube than the one which is orthogonal. In **b** and **c**, the orientation of the ellipsoid is non-collinear to the tube axis. Moreover in **c,** the tube axis and the molecule easy axis are parallel, yielding a very weak signal. This was confirmed by other samples and it suggests that the interaction is stronger when the molecule is flat-landing on the nanotube, as shown in the figures **a** and **d**.

4- Influence of the field sweep rate and the Landau-Zener tunnel probability

The sweeping rate is an important parameter to access to the dynamics of a magnetic system. Our measurements show that the switching field of the molecule experiencing a direct relaxation process is strongly dependent on the field sweep rate, as expected for the stochastic nature of the direct relaxation process (Fig. S4a). The Landau Zener theory predicts that the tunnel probability increases with decreasing sweep rate (Fig. S4b):

$$P_{m,m'} = 1 - \exp\left[-\frac{\pi\Delta^2_{m,m'}}{2\hbar g\mu_B|m - m'|\mu_0 \frac{dH_z}{dt}}\right]$$

Here m and m' are the quantum numbers of the avoided level crossing, Δ is the so-called tunnel splitting, dHz / dt is the magnetic field sweep rate, and *h-bar* is the Planck's constant. As a result, by decreasing the sweeping rate, more and more molecules should tunnel close to zero-field as shown in Figure 3b of the main text.

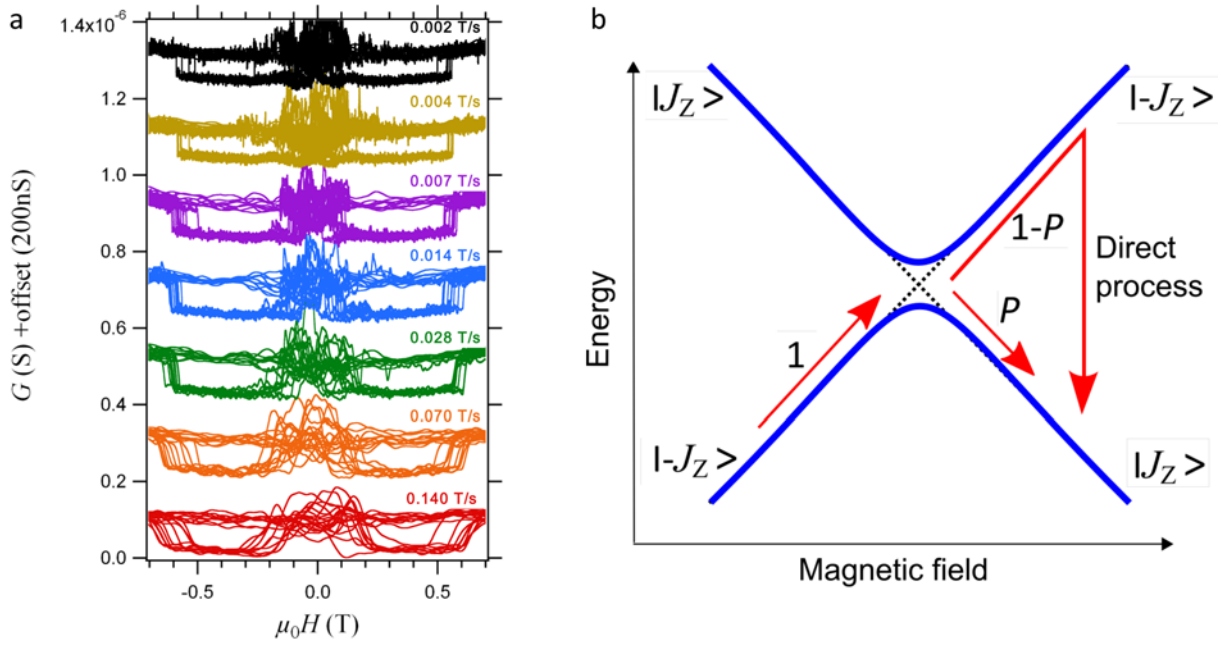

Figure S4: Splitting tunnel versus direct relaxation process. a, Hysteresis curves for different sweeping rates. For the trace, the magnetic field is swept from -0.7 T to -0.1 T at 140 mTs^{-1} and then the sweeping rate is changed to the announced value until the magnetic field reaches 0.7 T. For the retrace the opposite protocol is used. **b**, Illustration of the Landau-Zener theory. The magnetization is saturated to $-J_z$ and then the magnetic field is swept at a fixed velocity. The magnetization can tunnel either at zero field or at higher field by emitting a phonon. The tunnel probability **P** is given by the Landau-Zener formula.

DOI: 10.1038/NMAT3050

5- Temperature dependence of the switching field

The temperature dependence of the conductance hysteresis loops of the sample in Figure S2c is plotted in Figure S5. It shows a blocking temperature well above 1 K.

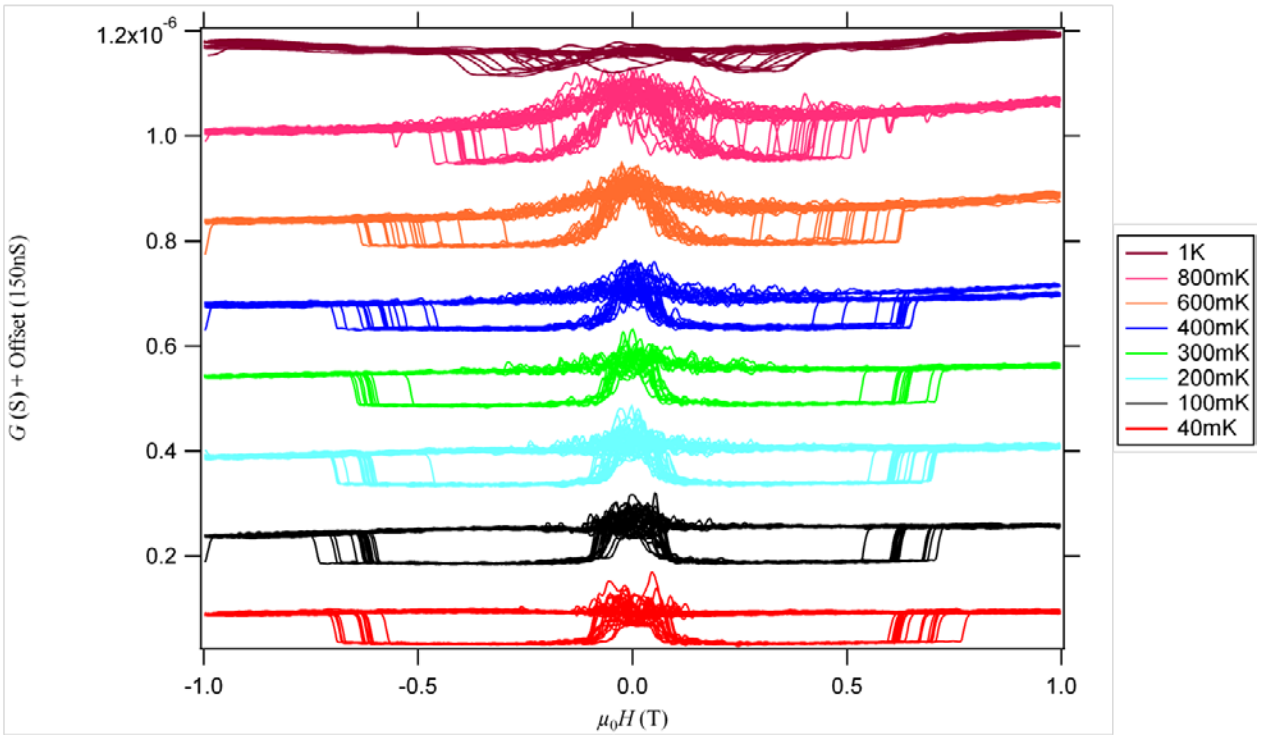

Figure S5: Temperature dependence of the conductance hysteresis loops corresponding to the same sample as in Fig. S2c. The field sweep rate is 60 mTs^{-1}.

6- Discussion about the magneto-Coulomb effect

The argumentation concerning the dismissal of magneto-Coulomb effects is the following: The Zeeman energy released by the molecule during the magnetic moment reversal could modify the chemical potential of the nanotube, see van der Molen et al. « Magneto-Coulomb effect in spin-valve devices » Physical Review B., 73(22):1-4 (2006). A shift of the Coulomb diamond is expected at the magnetisation reversal, as shown by Fig S6-a. Let's consider the case where a Coulomb peak moves toward the lower gate value, Fig S6-b. If we measure the magnetoconductance on the right part of the Coulomb peak, the magnetoconductance should be negative whereas if we measure it on the left part, it should be positive as shown on the Fig S6-c, d. As a consequence, the color on the Figure 2d should change on the top of a Coulomb peak. Since it doesn't, this kind of interpretation cannot be true. We can conclude that the Zeeman energy released is too small to perceptibly change the chemical potential.

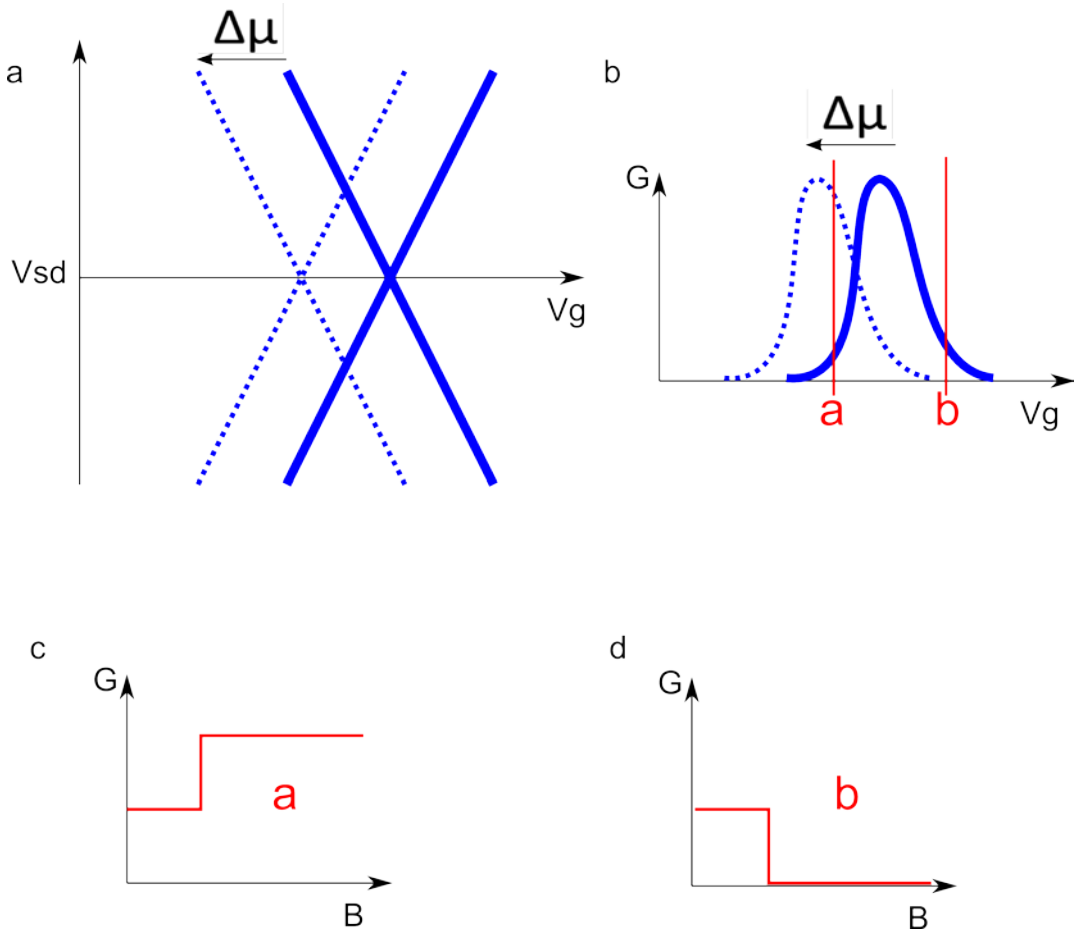

Figure S6: Scheme of the magneto-Coulomb effect on the conductance. When the chemical potential of the nanotube is modified by the magnetization reversal, the conductance drops down on the right slope of the initial Coulomb peak and increases on the left slope.